Unified description of passive vibration control for buildings based on pole allocation applied to 3-DOF model

Yoshiki IKEDA* and Yuki MATSUMOTO**

* Corresponding author
Disaster Prevention Research Institute, Kyoto University
Address: Gokasho, Uji, Kyoto 611-0011, JAPAN
TEL: +81-774-38-4086, FAX: +81-774-38-4334, E-mail: ikeda.yoshiki.6r@kyoto-u.ac.jp
** Graduate School of Engineering, Kyoto University

SUMMARY

For a building with a passive control system, an inverse problem is formulated based on the pole allocation method in control theory. The structural system is simplified as a three-degree-of-freedom lumped-mass damped shear model. Through the selection of appropriate model parameters, the simplified model can represent an earthquake-resistant structure, a base-isolated structure, an inter-storey-isolated structure, or a controlled structure with a tuned mass damper or viscous dampers. The natural frequencies and corresponding damping ratios in the three vibration modes are set as the initial control targets for the performance-based design. The newly introduced closed-form expression explains how the model parameters are related to the control target and generally proves the trade-off relationship in the passive control effect. Numerical examples demonstrate that pole allocation is arbitrary in selecting a solution. Nevertheless, only a limited solution can be applied to an actual building.

KEY WORDS

building, passive vibration control, unified understanding, pole allocation, performance-based design, 3-DOF

1. INTRODUCTION

A fundamental equation governing the passive vibration control of buildings is introduced through the application of pole allocation to a three-degree-of-freedom (3-DOF) lumped-mass damped shear model. A similar mathematical formulation was first introduced for a 3-DOF building model with inter-storey seismic isolation to elucidate its moderately complex dynamic behaviour [1]. A similar formulation was then extended to a 3-DOF model with base seismic isolation or tuned mass damper (TMD) [2,3]. In these studies, the base or inter-storey seismic isolation utilised analytical models that had a dashpot only in an isolation storey, whereas the TMD utilised a model that had both a spring and a dashpot linked with an auxiliary mass. Research studies have applied pole allocation to individually different models that express base

isolation, inter-storey isolation, or TMD. Each model had only one dashpot, which strongly influenced the dynamic nature of the corresponding structural system. Pole allocation was also applied to a 2-DOF simplified model with base isolation or TMD to easily reveal the control effect. As a result, the research series determined that there is a single governing equation independent of the analytical models for seismic isolation and TMD. The governing equation shows that the model parameters are automatically constrained by the assignment of three target modal properties. For the inter-storey isolation, the constraint indicates a trade-off relationship in the control effect between the upper and the lower sub-structures.

This advanced study applies pole allocation to a 3-DOF model with one dashpot in each storey to increase the modelling generality in the mathematical formulation. The newly introduced formulation proves that there is a general and significant governing equation for earthquake-resistant buildings and passively controlled buildings, which can also account for seismic isolation. The numerical examples in this study focus on a structural system with inter-storey dampers, because the formulation makes it possible to consider a design with passive-control dampers installed in all storeys. The results indicate that pole allocation is arbitrary in selecting a solution, and that only a limited solution can be applied to actual buildings.

Performance-based structural designs for buildings involve not only elastic response control for small/medium earthquakes but also elastic-plastic response control for large earthquakes. For example, FEMA 356, which is a first-generation performance-based design published in 2000, classifies the standard structural performance into four levels: Operational Performance Level, Immediate Occupancy Performance Level, Life Safety Performance Level, and Collapse Prevention Performance Level [4]. The guideline relates these levels to the peak inter-storey deformation angles, which are highly correlated with structural damage. To decrease the repair effort after a large earthquake, structural control technologies have been expected to be able to control, as much as possible, the seismic responses during an earthquake within the elastic ranges of structural members [5, 6]. Even if the performance-based design is advanced further in the future, structural control within the elastic range will continue to be studied at the initial design stage.

Equivalently linearised modelling is useful for understanding the nonlinear vibration of earthquake-resistant structures [7, 8]. The equivalent natural periods and damping ratios, depending on the seismic response amplitudes, are often incorporated in the present structural design. Equivalent linearisation is also used to evaluate the basic dynamic properties of seismic isolators and dampers. In structural design using seismic isolation, it is important to evaluate the equivalent natural period and damping ratio of an isolator responding to its shear strain [9]. Even in designs using displacement-dependent nonlinear hysteresis dampers, their energy dissipation effect is often evaluated as the equivalent damping ratio [10]. In system identification based on earthquake response records, the time-variant modal properties are examined to determine the dynamic performance of earthquake-resistant structures, seismically isolated structures and actively/passively controlled structures [11-14]. Pole allocation is consistent with performance-based design and structural control under linear or equivalently linear assumptions, because the modal properties, such as natural periods and their corresponding damping ratios, are set to be the target for controlling the structural response.

Pole allocation first places the closed-loop poles associated with the modes to be controlled on the left half of the complex plane to ensure the asymptotic stability of the system and then computes the linear feedback gains required to produce these poles [15, 16]. This approach is classified as a modern control theory that clearly sets the control criteria. Most past research on pole allocation has attracted interest in calculating feedback gains, which supposes its applications to active/semi-active control. At the dawn of the active control of civil engineering structures, it was introduced as a methodology for obtaining a feedback control algorithm [17].

Pole allocation has been applied in a variety of forms in the field of civil engineering. An application to active control in the lateral and torsional directions via only one control force indicates that the response reduction effect depends on the location of the controller, even if the same poles are assigned [18]. With pole allocation, it is always possible to assign the closed-loop poles of a linear time-invariant system. However, another application to an active mass damper leads to variable feedback gains, to account for stroke limitation [19]. Active control using non-resonance theory selects suitable closed-loop poles based on an analysis of the coming earthquake to avoid resonance and obtain a sufficient damping effect [20]. A similar application is determined from numerical simulations of semi-active dampers with a small amount of required control forces [21]. Multi-modal structural control combines a pole-placement controller with an integral resonant controller [22]. The pole-placement controller achieves a target equivalent modal viscous damping in the system and helps in the suppression of higher modes. The integral resonant controller reduces low-frequency vibrations caused by broad-band turbulent wind excitations.

Pole allocation seems to be applicable not only to active/semi-active control but also to passive control, because it assigns the natural frequencies and damping ratios of a controlled system. A viscous fluid passive energy dissipation system places the structural poles based on a modification of structural stiffness and the addition of a passive control system [23, 24]. The system was proposed for designing optimum passive energy dissipation systems using active control algorithms. The passive control system is designed to result in structural properties that are close to those extracted from the actively controlled system. At present, there have been few studies in which pole allocation was applied to the passive control of buildings.

The controllability of an open-loop system is equivalent to the possibility of assigning an arbitrary set of poles to the transfer matrix of the closed-loop system formed via suitable linear feedback of the state [15, 25]. When pole allocation is applied to a linear controllable time-invariant system with multi-control-inputs, the feedback gain matrix for realising the desired pole placement will contain a redundant nature in which the gain matrix cannot be uniquely determined [15, 25, 26]. As a result, an additional constraint is required to select an applicable solution from the candidate solutions. An example is the procedure used to search for a low feedback gain matrix [26]. When pole allocation is applied to a passively controlled structure, this arbitrariness problem occurs as a phenomenon in which the model parameters cannot be uniquely determined.

Until now, in the field of control theory, pole allocation has pursued generality and universality in obtaining a linear feedback control for a multi-input-multi-output system. Because of the matrix-vector expression in theory, solving a pole allocation problem inevitably depends on numerical processes. Consequently, it is difficult to know the basic properties inherent to a control objective, which, in this study,

a controlled building. This study restricts the objective model within a 3-DOF lumped-mass damped shear model with a dashpot in parallel to the stiffness in each storey. Nevertheless, the newly introduced closed-form expression proves that there is a general and significant governing equation for earthquake-resistant buildings and passively controlled buildings.

Chapter 2 presents the fundamental equation governing the passive control of buildings using a 3-DOF model with high generality. Chapter 3 solves the pole-allocation problem based on an assumption of lumped-mass weights. When the problem is first treated as an undamped eigenvalue problem, the pole allocation process is divided into two sequential processes: The first process is to calculate the stiffness in each storey, and the second is to calculate damping coefficients representing dampers. This treatment is advantageous for solving this pole-allocation problem from the viewpoint of engineering applications. Chapter 4 focuses on passively controlled buildings with dampers installed in all storeys and elucidates the fundamental characteristics. Even if lumped-mass weights are assumed, the pole allocation mathematically provides multiple sets of solutions under the same modal target. This chapter recognizes that only a limited solution can be applied to an actual building and considers both the smoothing stiffness variance and positive damping coefficients. The phenomenon responds to the strong constraint of the model parameters and is related to the trade-off relationship between the parameters and control effect. Finally, Chapter 5 presents the summary and conclusions.

2. POLE ALLOCATION APPLIED TO 3DOF MODEL

The formulation considers a 3-DOF lumped-mass damped shear model, as shown in Figure 1. Each storey has a dashpot that is in parallel to the stiffness. In the figure, m_U, m_I, and m_L denote the upper lumped mass, the inter-storey lumped mass, and the lower lumped mass, respectively; k_U, k_I, and k_L denote the shear stiffness values of the upper storey, the inter storey, and the lower storey, respectively; and c_U, c_I, and c_L denote the damping coefficients corresponding to the storey stiffnesses.

Through the selection of appropriate model parameters, the simplified model can be used to represent an earthquake resistant building or a passively controlled building under a linear assumption. When the stiffness in the lower storey is extremely small, compared to the others, and the corresponding damping coefficient is larger than the others, the model expresses base seismic isolation. When a similar parameter operation is applied to in the inter storey, the model expresses inter-storey seismic isolation. If the upper lumped mass, stiffness, and dashpot are assumed to be an auxiliary mass, a spring, and a damper, respectively, the model represents a building equipped with a TMD. Previous research has assumed $c_U = c_D = 0$ for inter-storey isolation [1], $c_U = c_I = 0$ for base isolation, and $c_I = c_L = 0$ for TMD [2, 3].

2.1. State equation

When the structure is excited by seismic excitation, the equation of motion can be expressed as

$$\begin{bmatrix} m_U & 0 & 0 \\ 0 & m_I & 0 \\ 0 & 0 & m_L \end{bmatrix}\begin{Bmatrix} \ddot{x}_U \\ \ddot{x}_I \\ \ddot{x}_L \end{Bmatrix}+\begin{bmatrix} c_U & -c_U & 0 \\ -c_U & c_U+c_I & -c_I \\ 0 & -c_I & c_I+c_L \end{bmatrix}\begin{Bmatrix} \dot{x}_U \\ \dot{x}_I \\ \dot{x}_L \end{Bmatrix}+\begin{bmatrix} k_U & -k_U & 0 \\ -k_U & k_U+k_I & -k_I \\ 0 & -k_I & k_I+k_L \end{bmatrix}\begin{Bmatrix} x_U \\ x_I \\ x_L \end{Bmatrix} = -\begin{bmatrix} m_U & 0 & 0 \\ 0 & m_I & 0 \\ 0 & 0 & m_L \end{bmatrix}\begin{Bmatrix} 1 \\ 1 \\ 1 \end{Bmatrix}\ddot{y}_0 \tag{1}$$

where, x_U, x_I, and x_L are the displacements of the lumped masses relative to the base, and $\ddot{y}_0$ is the ground acceleration input to the structural system.

Here, ω_U is defined as the natural circular frequency of the upper storey, ω_I is defined as the natural circular frequency when the upper storey is assumed to be rigid, and ω_L is defined as the natural circular frequency when the upper storey and inter storey are assumed to be rigid; whereas h_U, h_I, and h_L are introduced as the damping ratios corresponding to the natural circular frequencies. Meanwhile, μ_U is defined as the ratio of the upper lumped mass to the inter-storey lumped mass, and μ_L is defined as the ratio of the total mass of the upper and inter-storey lumped masses to the lower lumped mass. Then, the natural circular frequencies, damping ratios and mass ratios are expressed as the follows:

$$\omega_U^2 = k_U / m_U, \quad \omega_I^2 = k_I /(m_U + m_I), \quad \omega_L^2 = k_L /(m_U + m_I + m_L) \tag{2}$$

$$2h_U\omega_U = c_U / m_U, \quad 2h_I\omega_I = c_I /(m_U + m_I), \quad 2h_L\omega_L = c_L /(m_U + m_I + m_L) \tag{3}$$

$$\mu_U = m_U / m_I, \quad \mu_L = (m_U + m_I)/ m_L \tag{4}$$

For analytical convenience, Equation (1) can be rewritten as

$$\begin{Bmatrix} \ddot{x}_U \\ \ddot{x}_I \\ \ddot{x}_L \end{Bmatrix}+\begin{bmatrix} 2h_U\omega_U & -2h_U\omega_U & 0 \\ -2\mu_U h_U\omega_U & 2\mu_U h_U\omega_U + 2(1+\mu_U)h_I\omega_I & -2(1+\mu_U)h_I\omega_I \\ 0 & -2\mu_L h_I\omega_I & 2\mu_L h_I\omega_I + 2(1+\mu_L)h_L\omega_L \end{bmatrix}\begin{Bmatrix} \dot{x}_U \\ \dot{x}_I \\ \dot{x}_L \end{Bmatrix} + \begin{bmatrix} \omega_U^2 & -\omega_U^2 & 0 \\ -\mu_U\omega_U^2 & \mu_U\omega_U^2 + (1+\mu_U)\omega_I^2 & -(1+\mu_U)\omega_I^2 \\ 0 & -\mu_L\omega_I^2 & \mu_L\omega_I^2 + (1+\mu_L)\omega_L^2 \end{bmatrix}\begin{Bmatrix} x_U \\ x_I \\ x_L \end{Bmatrix} = -\begin{Bmatrix} 1 \\ 1 \\ 1 \end{Bmatrix}\ddot{y}_0 \tag{5}$$

When the state vector is composed of the relative velocities and displacements, the corresponding state equation is

$$\begin{Bmatrix} \ddot{x}_U \\ \ddot{x}_I \\ \ddot{x}_L \\ \dot{x}_U \\ \dot{x}_I \\ \dot{x}_L \end{Bmatrix} = \begin{bmatrix} -2h_U\omega_U & 2h_U\omega_U & 0 \\ 2\mu_U h_U\omega_U & -2\mu_U h_U\omega_U - 2(1+\mu_U)h_I\omega_I & 2(1+\mu_U)h_I\omega_I \\ 0 & 2\mu_L h_I\omega_I & -2\mu_L h_I\omega_I - 2(1+\mu_L)h_L\omega_L \\ 1 & 0 & 0 \\ 0 & 1 & 0 \\ 0 & 0 & 1 \end{bmatrix} \begin{bmatrix} -\omega_U^2 & \omega_U^2 & 0 & \\ \mu_U\omega_U^2 & -\mu_U\omega_U^2 - (1+\mu_U)\omega_I^2 & (1+\mu_U)\omega_I^2 & \\ 0 & \mu_L\omega_I^2 & -\mu_L\omega_I^2 - (1+\mu_L)\omega_L^2 & \\ 0 & 0 & 0 & \\ 0 & 0 & 0 & \\ 0 & 0 & 0 & \end{bmatrix} \begin{Bmatrix} \dot{x}_U \\ \dot{x}_I \\ \dot{x}_L \\ x_U \\ x_I \\ x_L \end{Bmatrix} - \begin{Bmatrix} 1 \\ 1 \\ 1 \\ 0 \\ 0 \\ 0 \end{Bmatrix} \ddot{y}_0 \tag{6}$$

2.2. Characteristic equation for system

With the Laplace operator $s = i\omega$ (where ω is the circular frequency), the characteristic equation is derived from the system matrix in Equation (6):

$$\begin{vmatrix} -2h_U\omega_U - s & 2h_U\omega_U & 0 \\ 2\mu_U h_U\omega_U & -2\mu_U h_U\omega_U - 2(1+\mu_U)h_I\omega_I - s & 2(1+\mu_U)h_I\omega_I \\ 0 & 2\mu_L h_I\omega_I & -2\mu_L h_I\omega_I - 2(1+\mu_L)h_L\omega_L - s \\ 1 & 0 & 0 \\ 0 & 1 & 0 \\ 0 & 0 & 1 \end{vmatrix} \begin{matrix} -\omega_U^2 & \omega_U^2 & 0 \\ \mu_U\omega_U^2 & -\mu_U\omega_U^2 - (1+\mu_U)\omega_I^2 & (1+\mu_U)\omega_I^2 \\ 0 & \mu_L\omega_I^2 & -\mu_L\omega_I^2 - (1+\mu_L)\omega_L^2 \\ -s & 0 & 0 \\ 0 & -s & 0 \\ 0 & 0 & -s \end{matrix} = 0 \tag{7}$$

Then, the six-dimensional matrix in Equation (7) is defined as matrix A, which is divided into four three-dimensional sub-matrices, i.e. A_{11}, A_{12}, A_{21} and A_{22}:

$$A = \begin{bmatrix} A_{11} & A_{12} \\ A_{21} & A_{22} \end{bmatrix},$$

$$A_{11} = \begin{bmatrix} -2h_U\omega_U - s & 2h_U\omega_U & 0 \\ 2\mu_U h_U\omega_U & -2\mu_U h_U\omega_U - 2(1+\mu_U)h_I\omega_I - s & 2(1+\mu_U)h_I\omega_I \\ 0 & 2\mu_L h_I\omega_I & -2\mu_L h_I\omega_I - 2(1+\mu_L)h_L\omega_L - s \end{bmatrix} \tag{8}$$

$$A_{12} = \begin{bmatrix} -\omega_U^2 & \omega_U^2 & 0 \\ \mu_U\omega_U^2 & -\mu_U\omega_U^2 - (1+\mu_U)\omega_I^2 & (1+\mu_U)\omega_I^2 \\ 0 & \mu_L\omega_I^2 & -\mu_L\omega_I^2 - (1+\mu_L)\omega_L^2 \end{bmatrix}, \quad A_{21} = \begin{bmatrix} 1 & 0 & 0 \\ 0 & 1 & 0 \\ 0 & 0 & 1 \end{bmatrix}, \quad A_{22} = \begin{bmatrix} -s & 0 & 0 \\ 0 & -s & 0 \\ 0 & 0 & -s \end{bmatrix}$$

The determinant of matrix A can be calculated using the following sub-matrices:

$$|A| = |A_{22}|\left|A_{11} - A_{12}A_{22}^{-1}A_{21}\right| \tag{9}$$

As a result, the determinant is expressed in polynomial form:

$$\begin{aligned}
&s^6 + 2[(1+\mu_U)h_U\omega_U + (1+\mu_U+\mu_L)h_I\omega_I + (1+\mu_L)h_L\omega_L]s^5 \\
&\quad + [(1+\mu_U)\omega_U^2 + (1+\mu_U+\mu_L)\omega_I^2 + (1+\mu_L)\omega_L^2 \\
&\qquad + 4(1+\mu_U)(1+\mu_L)(h_Uh_I\omega_U\omega_I + h_Ih_L\omega_I\omega_L + h_Uh_L\omega_U\omega_L)]s^4 \\
&\quad + 2(1+\mu_U)(1+\mu_L)[h_U\omega_U(\omega_I^2+\omega_L^2) + h_I\omega_I(\omega_L^2+\omega_U^2) + h_L\omega_L(\omega_U^2+\omega_I^2) + 4h_Uh_Ih_L\omega_U\omega_I\omega_L]s^3 \\
&\quad + (1+\mu_U)(1+\mu_L)[\omega_U^2\omega_I^2 + \omega_I^2\omega_L^2 + \omega_L^2\omega_U^2 + 4\omega_U\omega_I\omega_L(h_Uh_I\omega_L + h_Ih_L\omega_U + h_Lh_U\omega_I)]s^2 \\
&\quad + 2(1+\mu_U)(1+\mu_L)\omega_U\omega_I\omega_L(h_U\omega_I\omega_L + h_I\omega_L\omega_U + h_L\omega_U\omega_I)s + (1+\mu_U)(1+\mu_L)\omega_U^2\omega_I^2\omega_L^2 = 0
\end{aligned} \tag{10}$$

2.3. Characteristic equation for assigned poles

Under practical circumstances, the analytical model has three sets of conjugate poles. For the control target in the *i*-th mode, ω_i and h_i are defined as the natural circular frequency and the corresponding damping ratio, respectively. Then, the characteristic equation for the assigned poles is

$$\prod_{i=1}^{3}(s^2 + 2h_i\omega_i s + \omega_i^2) = 0 \tag{11}$$

This equation can be rewritten in the following polynomial form:

$$\begin{aligned}
&s^6 + 2(h_1\omega_1 + h_2\omega_2 + h_3\omega_3)s^5 + [4(h_1h_2\omega_1\omega_2 + h_2h_3\omega_2\omega_3 + h_3h_1\omega_3\omega_1) + \omega_1^2 + \omega_2^2 + \omega_3^2]s^4 \\
&\quad + 2[h_1\omega_1(\omega_2^2+\omega_3^2) + h_2\omega_2(\omega_3^2+\omega_1^2) + h_3\omega_3(\omega_1^2+\omega_2^2) + 4h_1h_2h_3\omega_1\omega_2\omega_3]s^3 \\
&\quad + [4\omega_1\omega_2\omega_3(h_1h_2\omega_3 + h_2h_3\omega_1 + h_3h_1\omega_2) + \omega_1^2\omega_2^2 + \omega_2^2\omega_3^2 + \omega_3^2\omega_1^2]s^2 \\
&\quad + 2\omega_1\omega_2\omega_3(h_1\omega_2\omega_3 + h_2\omega_3\omega_1 + h_3\omega_1\omega_2)s + \omega_1^2\omega_2^2\omega_3^2 = 0
\end{aligned} \tag{12}$$

2.4. Pole allocation

The characteristic equation, Equation (10), must be designed to be equal to the target characteristic equation, Equation (12), which requires the following parameter relationships:

$$(1+\mu_U)h_U\omega_U + (1+\mu_U+\mu_L)h_I\omega_I + (1+\mu_L)h_L\omega_L = h_1\omega_1 + h_2\omega_2 + h_3\omega_3 \tag{13}$$

$$\begin{aligned}
&(1+\mu_U)\omega_U^2 + (1+\mu_U+\mu_L)\omega_I^2 + (1+\mu_L)\omega_L^2 + 4(1+\mu_U)(1+\mu_L)(h_Uh_I\omega_U\omega_I + h_Ih_L\omega_I\omega_L + h_Uh_L\omega_U\omega_L) \\
&= 4(h_1h_2\omega_1\omega_2 + h_2h_3\omega_2\omega_3 + h_3h_1\omega_3\omega_1) + \omega_1^2 + \omega_2^2 + \omega_3^2
\end{aligned} \tag{14}$$

$$\begin{aligned}
&(1+\mu_U)(1+\mu_L)[h_U\omega_U(\omega_I^2+\omega_L^2) + h_I\omega_I(\omega_L^2+\omega_U^2) + h_L\omega_L(\omega_U^2+\omega_I^2) + 4h_Uh_Ih_L\omega_U\omega_I\omega_L] \\
&= h_1\omega_1(\omega_2^2+\omega_3^2) + h_2\omega_2(\omega_3^2+\omega_1^2) + h_3\omega_3(\omega_1^2+\omega_2^2) + 4h_1h_2h_3\omega_1\omega_2\omega_3
\end{aligned} \tag{15}$$

$$\begin{aligned}
&(1+\mu_U)(1+\mu_L)[\omega_U^2\omega_I^2 + \omega_I^2\omega_L^2 + \omega_L^2\omega_U^2 + 4\omega_U\omega_I\omega_L(h_Uh_I\omega_L + h_Ih_L\omega_U + h_Lh_U\omega_I)] \\
&= 4\omega_1\omega_2\omega_3(h_1h_2\omega_3 + h_2h_3\omega_1 + h_3h_1\omega_2) + \omega_1^2\omega_2^2 + \omega_2^2\omega_3^2 + \omega_3^2\omega_1^2
\end{aligned} \tag{16}$$

$$(1+\mu_U)(1+\mu_L)\omega_U\omega_I\omega_L(h_U\omega_I\omega_L+h_I\omega_L\omega_U+h_L\omega_U\omega_I)=\omega_1\omega_2\omega_3(h_1\omega_2\omega_3+h_2\omega_3\omega_1+h_3\omega_1\omega_2) \tag{17}$$

$$(1+\mu_U)(1+\mu_L)\omega_U^2\omega_I^2\omega_L^2=\omega_1^2\omega_2^2\omega_3^2 \tag{18}$$

These equations have eight unknown design parameters to be solved: ω_U, ω_I, ω_L, h_U, h_I, h_L, μ_U, and μ_L. Dividing Equation (17) by Equation (18) yields the following significant relationship:

$$\frac{h_U}{\omega_U}+\frac{h_I}{\omega_I}+\frac{h_L}{\omega_L}=\frac{h_1}{\omega_1}+\frac{h_2}{\omega_2}+\frac{h_3}{\omega_3} \tag{19}$$

In past research by the authors, it was assumed that a 3-DOF model has one dashpot in only one storey: For inter-storey seismic isolation, $h_U=h_L=0$ is assumed in Equation (19); for base seismic isolation, $h_U=h_I=0$; and for TMD, similarly, $h_I=h_L=0$. With high generality, Equation (19) integrates an earthquake-resistant structure and passively controlled structures (including three control systems) into one system. The equation illustrates the trade-off relationship among the three terms on the left side, because the right side becomes constant after the target modal properties ω_i and h_i are determined.

2.5. Independence of trade-off relationship from parameter definition

The previous sections define ω_I and ω_L as the natural circular frequencies when the storeys above the objective storey are assumed to be rigid, h_I and h_L as the damping ratios corresponding to these frequencies. This section introduces new parameter definitions as follows:

$$\omega_{I*}^2=k_I/m_I,\quad \omega_{L*}^2=k_L/m_L \tag{20}$$

$$2h_{I*}\omega_{I*}=c_I/m_I,\quad 2h_{L*}\omega_{L*}=c_L/m_L \tag{21}$$

where, ω_{I*} and h_{I*} are the natural circular frequency and damping ratio for an S-DOF model with an inter-storey lumped mass, wherein the inter storey is considered as the objective storey. Similarly, ω_{L*} and h_{L*} are the corresponding parameters for another S-DOF model with the lower lumped mass, wherein the lower storey is considered as the objective storey.

$$\omega_I=\sqrt{\frac{m_I}{m_U+m_I}}\omega_{I*}=\frac{\omega_{I*}}{\sqrt{1+\mu_U}},\quad h_I=\frac{2h_{I*}\omega_{I*}}{2\sqrt{1+\mu_U}\,\omega_{I*}}=\frac{h_{I*}}{\sqrt{1+\mu_U}} \tag{22}$$

$$\omega_L=\sqrt{\frac{m_L}{m_U+m_I+m_L}}\omega_{L*}=\frac{\omega_{L*}}{\sqrt{1+\mu_L}},\quad h_L=\frac{2h_{L*}\omega_{L*}}{2\sqrt{1+\mu_L}\,\omega_{L*}}=\frac{h_{L*}}{\sqrt{1+\mu_L}} \tag{23}$$

Substituting Equations (22) and (23) into Equation (19) yields a similar relationship:

$$\frac{h_U}{\omega_U}+\frac{h_I}{\omega_I}+\frac{h_L}{\omega_L}=\frac{h_U}{\omega_U}+\frac{h_{I*}}{\omega_{I*}}+\frac{h_{L*}}{\omega_{L*}}=\frac{h_1}{\omega_1}+\frac{h_2}{\omega_2}+\frac{h_3}{\omega_3} \tag{24}$$

This proves that the trade-off relationship is independent of the parameter definitions in expressing an equation of motion.

To easily determine the passive control when a damper is installed in each storey, Equations (13) to (18) are rewritten via substitution by Equations (22) and (23):

$$(1+\mu_U)h_U\omega_U + (1+\mu_3)h_{I^*}\omega_{I^*} + h_{L^*}\omega_{L^*} = h_1\omega_1 + h_2\omega_2 + h_3\omega_3 \tag{25}$$

$$\begin{aligned}&(1+\mu_U)\omega_U^2 + (1+\mu_3)\omega_{I^*}^2 + \omega_{L^*}^2 + 4[(1+\mu_L)h_U h_{I^*}\omega_U\omega_{I^*} + h_{I^*}h_{L^*}\omega_{I^*}\omega_{L^*} + (1+\mu_U)h_U h_{L^*}\omega_U\omega_{L^*}] \\ &= 4(h_1h_2\omega_1\omega_2 + h_2h_3\omega_2\omega_3 + h_3h_1\omega_3\omega_1) + \omega_1^2 + \omega_2^2 + \omega_3^2\end{aligned} \tag{26}$$

$$\begin{aligned}&h_U\omega_U[(1+\mu_L)\omega_{I^*}^2 + (1+\mu_U)\omega_{L^*}^2] + h_{I^*}\omega_{I^*}[\omega_{L^*}^2 + (1+\mu_D)\omega_U^2] + h_{L^*}\omega_{L^*}[(1+\mu_U)\omega_U^2 + \omega_{I^*}^2] + 4h_U h_{I^*}h_{L^*}\omega_U\omega_{I^*}\omega_{L^*} \\ &= h_1\omega_1(\omega_2^2 + \omega_3^2) + h_2\omega_2(\omega_3^2 + \omega_1^2) + h_3\omega_3(\omega_1^2 + \omega_2^2) + 4h_1h_2h_3\omega_1\omega_2\omega_3\end{aligned} \tag{27}$$

$$\begin{aligned}&(1+\mu_L)\omega_U^2\omega_{I^*}^2 + \omega_{I^*}^2\omega_{L^*}^2 + (1+\mu_U)\omega_{L^*}^2\omega_U^2 + 4\omega_U\omega_{I^*}\omega_{L^*}(h_U h_{I^*}\omega_{L^*} + h_{I^*}h_{L^*}\omega_U + h_{L^*}h_U\omega_{I^*}) \\ &= 4\omega_1\omega_2\omega_3(h_1h_2\omega_3 + h_2h_3\omega_1 + h_3h_1\omega_2) + \omega_1^2\omega_2^2 + \omega_2^2\omega_3^2 + \omega_3^2\omega_1^2\end{aligned} \tag{28}$$

$$\omega_U\omega_{I^*}\omega_{L^*}(h_U\omega_{I^*}\omega_{L^*} + h_{I^*}\omega_{L^*}\omega_U + h_{L^*}\omega_U\omega_{I^*}) = \omega_1\omega_2\omega_3(h_1\omega_2\omega_3 + h_2\omega_3\omega_1 + h_3\omega_1\omega_2) \tag{29}$$

$$\omega_U^2\omega_{I^*}^2\omega_{L^*}^2 = \omega_1^2\omega_2^2\omega_3^2 \tag{30}$$

where

$$\mu_3 = \frac{m_I}{m_L} = \frac{\dfrac{m_U + m_I}{m_L}}{\dfrac{m_U + m_I}{m_I}} = \frac{\mu_L}{1+\mu_U} \tag{31}$$

3. NUMERICAL ANALYSIS WITH APPROXIMATION OF LOW DAMPING

This study focuses on pole allocation when three lumped masses are known *a priori*. This problem involves determining three natural circular frequencies (ω_U, ω_{I^*}, and ω_{L^*}) and three damping ratios (h_U, h_{I^*}, and h_{L^*}) for fixed mass ratios (μ_U and μ_L). In other words, the objective is to determine the stiffness values and damping coefficients for the three storeys.

Equations (25) to (30) have many high-order terms that consist of six unknown parameters (ω_U, ω_{I^*}, ω_{L^*}, h_U, h_{I^*}, and h_{L^*}). From the viewpoint of applicability, the three natural circular frequencies are first obtained via approximation of the damped 3-DOF system as an undamped 3-DOF system. This approximation is acceptable because the effect of less than 20% damping ratio is much smaller in calculation for the natural frequencies of the structure. In an S-DOF system with 20% damping ratio, the damped natural frequency is 98.0% of the corresponding undamped natural frequency.

Neglecting the target damping ratios (h_1, h_2, and h_3) and the products of the structural damping ratios leads to the following simplified equations from Equations (26), (28) and (30):

$$(1+\mu_U)\omega_U^2 + (1+\mu_3)\omega_{I^*}^2 + \omega_{L^*}^2 = (1+b^2+c^2)\omega_1^2 \tag{32}$$

$$(1+\mu_D)\omega_U^2\omega_{I^*}^2 + \omega_{I^*}^2\omega_{L^*}^2 + (1+\mu_U)\omega_{L^*}^2\omega_U^2 = (b^2 + b^2c^2 + c^2)\omega_1^4 \tag{33}$$

$$\omega_U^2\omega_{I*}^2\omega_{L*}^2 = b^2c^2\omega_1^6 \tag{34}$$

where the non-dimensional parameters b and c are the ratios of the second and third natural frequencies to the first one, respectively:

$$b = \omega_2 / \omega_1, \quad c = \omega_3 / \omega_1 \tag{35}$$

Similarly, Equations (32), (33), and (34) can be rewritten using other non-dimensional parameters (x , y , and z):

$$(1+\mu_L)x + (1+\mu_3)y + z = 1 + b^2 + c^2 \tag{36}$$

$$(1+\mu_L)xy + yz + (1+\mu_U)zx = b^2 + b^2c^2 + c^2 \tag{37}$$

$$xyz = b^2c^2 \tag{38}$$

where

$$x = \omega_U^2 / \omega_1^2 = f_U^2 / f_1^2, \quad y = \omega_{I*}^2 / \omega_1^2 = f_{I*}^2 / f_1^2, \quad z = \omega_{L*}^2 / \omega_1^2 = f_{L*}^2 / f_1^2 \tag{39}$$

Here, f_U , f_{I*}, and f_{L*} are the natural frequencies corresponding to ω_U , ω_{I*}, and ω_{L*}, respectively.

Next, h_U , h_{I*}, and h_{L*} are calculated based on Equation (40) using x , y , and z obtained from Equations (36) to (38):

$$\begin{Bmatrix} h_U \\ h_{I*} \\ h_{D*} \end{Bmatrix} = \begin{bmatrix} (1+\mu_U)\sqrt{x} & (1+\mu_3)\sqrt{y} & \sqrt{z} \\ \sqrt{x}\{(1+\mu_L)y + (1+\mu_U)z\} & \sqrt{y}\{z + (1+\mu_L)x\} & \sqrt{z}\{(1+\mu_U)x + y\} \\ \sqrt{x}yz & x\sqrt{yz} & xy\sqrt{z} \end{bmatrix}^{-1} \begin{Bmatrix} h_1 + bh_2 + ch_3 \\ (b^2+c^2)h_1 + b(1+c^2)h_2 + c(1+b^2)h_3 \\ bc(bch_1 + ch_2 + bh_3) \end{Bmatrix} \tag{40}$$

This approximation divides the six simultaneous equations into two sets of three simultaneous equations, which is an advantage in solving this pole-allocation problem from the viewpoint of engineering applicability.

Now, we attempt to numerically and easily solve the equation set (36) to (38) with unknown second-/three-order variables. Equation (36) is transformed into Equation (41):

$$z = 1 + b^2 + c^2 - (1+\mu_U)x - (1+\mu_3)y \tag{41}$$

The equation is substituted into Equations (37) and (38):

$$(1+\mu_U)^2x^2 + \{(1+2\mu_U)y - (1+\mu_U)(1+b^2+c^2)\}x - (1+b^2+c^2)y + (1+\mu_3)y^2 + b^2 + b^2c^2 + c^2 = 0 \tag{42}$$

$$y=\frac{(1+b^2+c^2)x-(1+\mu_U)x^2 \pm \sqrt{[(1+b^2+c^2)x-(1+\mu_U)x^2]^2-4(1+\mu_3)b^2c^2x}}{2(1+\mu_3)x} \tag{43}$$

After ω_1, b and c are set, the solving process have four steps: Step 1 is to assume the range of x and, from this range, select a certain x; Step 2 is to calculate y using Equation (43); Step 3 is to check whether x satisfies Equation (42), and if x satisfies the equation, it is a solution; and Step 4 is to return to Step 1 or 2 if x does not satisfy Equation (42).

Similarly, Equation (44) can be obtained from Equation (42); y is assumed for the numerical solving process.

$$x=\frac{(1+b^2+c^2)y-(1+\mu_3)y^2 \pm \sqrt{[(1+b^2+c^2)y-(1+\mu_3)y^2]^2-4(1+\mu_U)b^2c^2y}}{2(1+\mu_U)y} \tag{44}$$

Equations (43) and (44) imply that the pole allocation has multiple solutions, which will be explained in a later chapter.

4. CHARACTERISTICS IN APPLICATION TO INTER-STOREY PASSIVE DAMPERS

Chapter 4 presents an investigation of the fundamental characteristics of the newly introduced pole allocation in an application involving passive dampers installed in all storeys of a building. All numerical examples assume that the three lumped-mass weights are the same, i.e. $\mu_U = 1$ and $\mu_L = 2$.

4.1. Natural frequencies

From the viewpoint of natural frequencies, the existence of solutions for the simultaneous Equations (36) to (38) is investigated for the region where the frequency ratio b ranges from 2.0 to 3.0 and the other frequency ratio c ranges from 3.5 to 5.0. The frequency ratios b and c are then varied in increments of 0.01, as shown in Figure 2, and the numerical characteristic is searched for an area where a set of solutions *x*, *y* and *z* exists. This area occurs where c is greater than 3.74. In the figure, the area is marked by three types of squares (grey filled, grey unfilled, and red filled) and one type of rhombus (blue unfilled). As described in the figure legend, the grey filled squares indicate the points at which two sets of solutions exist, whereas the red filled squares indicate the points at which four sets of solutions exist. The area occupied by the grey filled squares is large, whereas the area occupied by the red squares is much smaller. The grey filled squares mostly occupy the existing solution area.

In a standard building, the shear stiffness values tend to decrease in the upper storeys. In the figure, each point where at least one set of solutions matches this tendency is marked by a grey unfilled square, defined as ‘Gradually decreasing’ in the figure legend. The corresponding area appears as dark grey. The dark grey region satisfies the inequality $x < y < z$ because the three lumped masses have the same values. The blue

rhombus, noting '−20% to 0% decreasing', indicates each point at which the non-dimensional x and y are within 80%−100% of y and z, respectively. The blue area mathematically satisfies two inequalities, i.e. $0.8\sqrt{y} \le \sqrt{x} \le 1.0\sqrt{y}$ and $0.8\sqrt{z} \le \sqrt{y} \le 1.0\sqrt{z}$, which indicates that the stiffness change is smoothed in the height direction from a practical viewpoint. The black point located at $b = 2.635$ and $c = 3.876$ (i.e. average values for the blue rhombuses) marks the centre of the blue area. Although we can mathematically determine multiple sets of natural circular frequencies (ω_U, ω_{I*}, and ω_{L*}) satisfying the target pole locations, only a limited solution can be applied to an actual building. Multiple sets of solutions respond to arbitrariness when pole allocation is applied to secure linear feedback gains for a controlled system [15, 25, 26].

Based on a selection of four cases, i.e. $b = 2.40$, $b = 2.60$, $c = 3.90$, and $c = 4.95$ from Figure 2, the solution characteristics are then studied using three non-dimensional frequencies such as $\sqrt{x} = f_U / f_1$, $\sqrt{y} = f_{I*} / f_1$, and $\sqrt{z} = f_{L*} / f_1$. Figure 3 illustrates a case in which $b = 2.40$. The solutions exist within the range $3.85 \le c$. Black, red, and blue circles denote the non-dimensional natural frequencies of the upper storey, inter-storey, and lower storey, respectively. Two sets of solutions exist in the range $3.85 \le c \le 4.95$, whereas four sets exist in the small range $4.96 \le c \le 5.00$. The solution curves are drawn with colours and numbers to identify individual sets of solutions. Each number is used merely as a label for one set of solutions, whereas the numbering sequence has no meanings. For example, the yellow circles represent solution set 3, whereas the green circles represent solution set 4. When b is fixed at a certain value, the same number identifies one set of solutions. The two sets result in three curves with convex at $c = 3.85$ and three other curves with convex at $c = 4.96$. In the range $3.85 \le c \le 4.95$, the upper parts of the f_U / f_1 and f_{I*} / f_1 curves correspond to solution set 1, whereas the lower parts correspond solution set 2. In the same range, the upper part of f_{L*} / f_1 corresponds to solution set 2, whereas the lower part corresponds to solution set 1. On the other hand, in the range $4.96 \le c \le 5.00$, the solutions are of a complex nature. For the curves with convex at $c = 4.96$, the upper parts of f_U / f_1 and f_{L*} / f_1 correspond to solution set 1, whereas the lower part of f_{I*} / f_1 corresponds to solution set 3. Meanwhile, for the inter storey, the upper part corresponds to solution set 3, whereas the lower part corresponds to solution set 1. In the range $4.96 \le c \le 5.00$, solution set 2 occurs locally around the convex edges, whereas solution set 4 occurs on the curves with convex at $c = 3.85$.

Figure 4 illustrates a case in which $b = 2.60$. The solutions exist within the range $3.75 \le c$. This case always has two solution sets, and its nature is simple compared to the case presented in Figure 3. On the other hand, Figure 5 visualises a case in which $c = 3.90$. The solutions exist in the range $2.34 \le b$. Similar to the case presented in Figure 4, this case has two sets of solutions. When b becomes larger, the large–small relation of solution values between f_U / f_1 and f_{I*} / f_1 is reversed completely. Figure 6 shows a case in which $c = 4.95$. The solutions exist in the range $2.09 \le b$. In this case, four sets of solutions exhibit a complex phenomenon with the *S*-shape curves at approximately $b = 2.38$, and their appearances are different from those of the curves shown in Figure 3.

Based on a selection of two sets of solutions at $b = 2.60$ and $c = 3.90$ and an assumption of an undamped eigenvalue problem, Figure 7 illustrates the participation functions as mode shapes with

participation factors for input ground motion. The depicted mode shapes are not affected by the first natural frequency or the assumed mass weights. Figure 7 (a) corresponds to solution set 1, whereas Figure 7 (b) corresponds to solution set 2. For solution set 1, it seems that three natural frequencies can be obtained via adjustment of the modal amplitudes for all lumped-masses. On the other hand, for solution set 2, it seems that first and second natural frequencies are the first to be obtained via adjustment of the amplitudes for the upper and inter-storey lumped masses, after which the third natural frequency is obtained via adjustment of the amplitudes for all lumped masses. This inference may be supported by the fact, for the lower lumped mass (mass number 1), the first modal amplitude is nearly equal to the second modal amplitude. The mode shapes in Figure 7 (a) correspond to solutions satisfying the two inequalities $0.8\sqrt{y} \le \sqrt{x} \le 1.0\sqrt{y}$ and $0.8\sqrt{z} \le \sqrt{y} \le 1.0\sqrt{z}$, which indicate that the stiffness change is smoothed. By contrast, the mode shapes in Figure 7 (b) do not satisfy the inequality conditions.

The stiffness values of a building model can be calculated using Equations (2) and (20). Based on an assumption 1.0 Hz as the first natural frequency and 9.80665 × 10^3 kN (1,000 tf) as the weight of each lumped mass, Table 1 outlines the stiffness for each storey. These data confirm that the stiffness undergoes a smoothing change, which is natural from a practical viewpoint.

4.2. Damping ratios

Based on an assumption of an undamped eigenvalue problem, to obtain natural frequency solutions independently of structural damping, the six-dimensional simultaneous equations can be divided into two sets of three-dimensional simultaneous equations. The previous section focuses on the fundamental characteristics of the natural frequencies. Following the results, this section focuses on the control effect of the dampers. To make a building model consistent with engineering applications, its damping coefficients represented by dashpots should be positive instead of negative. For the numerical examples in this section, $b = 2.60$ and $c = 3.90$, which are the same parameters for the mode shapes shown in Figure 7. These parameters produce two sets of solutions for ($\sqrt{x} = f_U / f_1$, $\sqrt{y} = f_{I*} / f_1$, $\sqrt{z} = f_{L*} / f_1$), i.e. (1.938, 2.232, 2.344) and (1.697, 1.868, 3.199). The former is solution set 1, with practicability shown in Figures 4 and 5, whereas the latter is solution set 2, without practicability. The control effect is discussed only solution set 1.

Figure 8 shows combinations of three target modal damping ratios (h_1, h_2, and h_3) that produce positive values for the structural damping ratios (h_U, h_{I*}, and h_{L*}). Each target modal damping ratio h_i ($i = 1, 2, 3$) is varied from 0.01 to 0.20 in increments of 0.01. The horizontal coordinate indicates the target first damping ratio (h_1), whereas the vertical coordinate indicates the target second and third damping ratios (h_2 and h_3). The squares represent the relationship between h_1 and h_2, whereas the triangles represent the relationships between h_1 and h_3. The area where all the structural damping coefficients become positive is limited, and in which h_2 and h_3 are larger than h_1. As with the structural natural frequencies, only suitable structural damping ratios can be applied to an actual building. For the stiffness and damping that are to be applied in actual practice, a useful solution should be selected from among the candidate solutions obtained via the mathematical calculations.

For the case of $h_1 = 0.05$, Figures 9 and 10 visualise the structural damping ratios for the three storeys

(h_U, h_{I*}, and h_{L*}). As shown in Figure 8, all the structural damping ratios become positive when $0.06 \le h_2$. Figure 9 shows the case for $0.06 \le h_2 \le 0.10$, whereas Figure 10 shows the case for $0.11 \le h_2 \le 0.20$. The horizontal coordinates represent h_3. Although the sums of the three ratios ($h_U + h_{I*} + h_{L*}$) are always within the range 0.25 to 0.37, the damping distribution depends mainly on h_3. When h_2 is fixed at a certain value, a larger h_3 increases h_U for the upper storey and h_{I*} for the inter storey. This phenomenon can be explained by the mode shapes in Figure 7 (a), where an increasing in h_2 remarkably affects h_U because the second mode shape has the largest amplitude for the upper storey. Similarly, an increasing in h_3 affects h_{I*} because the third mode shape has the largest amplitude for the inter storey.

For the case of $h_1 = 0.10$, Figure 11 illustrates similar distributions for the structural damping ratios. More specifically, h_U, h_{I*}, and h_{L*} become positive when $0.17 \le h_2$. A similar tendency can be observed in the distributions. However, the damping ratios for the lower storey are larger than those shown in Figures 9 and 10, because the higher h_1 increases the effect of the first mode, which has the largest amplitude for the lower storey.

An unrealistic set of solutions is where at least one structural damping ratio (h_U, h_{I*}, or h_{L*}) becomes negative. In an unrealistic set of solutions, the target damping ratios are archived via an extreme increase in the positive damping ratio for a storey.

Finally, Equations (19) and (24), which express the trade-off relationship, can be interpreted geometrically. If the natural circular frequencies (ω_U, ω_{I*}, and ω_{L*}) are replaced with the corresponding natural frequencies (f_U, f_{I*}, and f_{L*}), Equation (24) can be rewritten as

$$\frac{h_U}{f_U} + \frac{h_{I*}}{f_{I*}} + \frac{h_{L*}}{f_{L*}} = d\,, \quad d = \sum_{i=1}^{3} \frac{h_i}{f_i}\,. \tag{45}$$

Solving the undamped eigenvalue problem described in Chapter 3 provides the values of f_U, f_{I*}, and f_{L*} before h_U, h_{I*}, and h_{L*} are calculated. This two-step calculation process fixes all denominators on the left side of Equation (45), whereas the corresponding numerators become variables. When the variables are plotted on a Cartesian coordinate system in three dimensions, the trade-off equation can be illustrated by the plane shown in Figure 12. The area with engineering applicability is $0 < h_U$, $0 < h_{I*}$ and $0 < h_{L*}$.

5. CONCLUSIONS

The fundamental equation governing a passively controlled building is derived through the application of pole allocation to a 3-DOF lumped-mass damped shear model. Based on a selection of approximate model parameters, the model can represent an earthquake-resistant structure, a base-isolated structure, an inter-storey-isolated structure, or a controlled structure with a TMD or viscous dampers. The newly introduced closed-form expression describes how the model parameters are related to the control target and generally proves the trade-off relationship in the passive control effect. Numerical examples demonstrate that the pole allocation is arbitrary in selecting a solution. Nevertheless, only a limited solution can be

applied to an actual building. The research results are summarised as follows:

1) Past research studies have applied pole allocation to individually different models that express base isolation, inter-storey isolation, or TMD. Each model had only one dashpot, which strongly influences the dynamic nature of the corresponding structural system. This study applies pole allocation to a general 3-DOF model that has one dashpot in each storey. With its high generality, the newly introduced closed-form trade-off relationship integrates earthquake-resistant buildings and passively controlled buildings, and can account for seismic isolation. This relationship indicates that the model parameters are automatically constrained by the assignment of three target modal properties. This relationship is not affected by the definition of the model parameters.
2) The pole allocation provides six simultaneous equations with eight unknown parameters to be solved. Based on an assumption of lumped-mass weights and through simplification of the problem into an undamped eigenvalue problem, the simultaneous equations can be divided into two sets of three simultaneous equations. As a result, the structural damping ratios can be evaluated after the stiffness values are determined. This approximation has the advantage of enabling pole allocation to be easily solved from the viewpoint of engineering applications. Through the decoupling of the structural damping ratios and stiffnesses in solving the problem, it becomes possible to infer the trade-off occurs in structural damping ratios. This inference can be expressed by an equation of a plane in Cartesian coordinates in three dimensions.
3) The pole allocation is arbitrary in mathematically determining the model parameters even if the target modal properties are the same and the lumped-mass weights are fixed. Nevertheless, a limited practical solution is selected based on two facts: the shear stiffness values become lower in the upper storeys, and the damping coefficients for a standard building have positive values. The areas where practical solutions exist are relatively small. For the realistic solutions, three natural frequencies are obtained via adjustment of the modal amplitudes for all lumped masses. On the other hand, for the unrealistic solutions, the first and second natural frequencies are first obtained via adjustment of the amplitudes for the upper and inter-storey lumped masses, after which the third natural frequency is obtained via adjustment of the amplitudes for all lumped masses.
4) Structural damping coefficients, referred to as the control effect, are strongly affected by the target model damping ratios and modal shapes. When the target modal damping ratios are larger in the second and third modes, it is easy to secure positive values for the structural damping coefficients.

ACKNOWLEDGEMENTS

This work was supported by JSPS KAKENHI (Grant Number 20K05027). The authors greatly appreciate the financial support provided.

REREFENCE

1. Ikeda Y. Fundamental equation based on pole allocation for interstory seismic isolation of buildings. *Structural Control and Health Monitoring* 2021; 28(3): 19 pages: article ID e2687.
2. Ikeda Y. Unified understanding of base seismic isolation, interstory seismic Isolation and tuned mass

damper for Buildings. *DPRI Annuals* 2021, Disaster Prevention Research Institute, Kyoto University; 64B: 21-39. https://www.dpri.kyoto-u.ac.jp/nenpo/no64/ronbunB/a64b0p03.pdf (in Japanese).

3. Matsumoto Y, Ikeda Y. Unified understanding of base seismic isolation, interstory seismic Isolation and tuned mass damper for Buildings. *Proceedings of the annual meeting* (s*tructures*) 2021 (ISSN 1345- 6660), *Kinki Branch*. *Architectural Institute of Japan*; 61: 341-344 (in Japanese).
4. FEMA (Federal Emergency Management Agency) 356. *Prestandard and Commentary for the Seismic Rehabilitation of Buildings*. American Society of Civil Engineers (ASCE); 2000.
5. Connor JJ, Wada A, Iwata M, Huang Y.H. Damage-controlled structures. I: Preliminary design methodology for seismically active regions. *Journal of Structural Engineering*, ASCE 1997; 123(4): 423-431.
6. Wada A, Shimizu K, Kawai H, Iwata M. Abe S. *Damage-Controlled Structure*. Maruzen Publishing; 1998 (in Japanese).
7. Caughey TK. Sinusoidal excitation of a system with bilinear hysteresis. *Journal of Applied Mechanics*, ASME 1960; 27(4): 640-643.
8. Caughey TK. Equivalent linearization techniques. *Journal of the Acoustical Society of America* 1963; 35(11): 1706-1711.
9. Kelly JM. *Earthquake-Resistant Design with Rubber*. *2nd edition*. Springer-Verlag London; 1997.
10. Soong TT, Dargush GF. *Passive Energy Dissipation Systems in Structural Engineering*. John Wiley & Sons; 1997.
11. Loh CH, Lin HM. Application of off-line and on-line identification techniques to building seismic response data. *Earthquake Engineering & Structural Dynamics* 1996; 25(3): 269-290.
12. Ikeda Y. Active and semi-active vibration control of buildings in Japan -Practical applications and verification-. *Structural Control and Health Monitoring* 2009; 16(7-8): 703-723.
13. Ikeda Y. Verification of system identification utilizing shaking table tests of a full-scale 4-story steel building. *Earthquake Engineering & Structural Dynamics* 2016; 45(4); 543-562.
14. Fujino Y, Siringoringo DM, Ikeda Y, Nagayama T, Mizutani T. Research and implementations of structural monitoring for bridges and buildings in Japan. *Engineering* 2019; 5(6); 1093-1119.
15. Wonham WM. On pole assignment in multi-input controllable linear systems, *IEEE Transactions on Automatic Control* 1967; 12(6): 660-665.
16. Meirovitch L. *Dynamics and Control of Structures*. John Wiley & Sons; 1990.
17. Leipholz HHE, Abdel-Rohman M. *Control of Structures*. Martinus-Nijhoff Publications; 1986.
18. Ikeda Y, Kobori T. Structure with uniaxial eccentricity actively controlled by only one control force. *Proceedings of the 1st world conference on Structural Control* 1994, International Association for Structural Control (ISBN 0-9628908-3-9); Pasadena, California, USA; 3: FP1 3-12.
19. Yamamoto M, Suzuki Y. Experimental study on seismic response control of full-scale structure based on pole assignment algorithm considering AMD with stroke limitation. *Journal of Structural and Construction Engineering* (*Transactions* of AIJ) 1998; 514: 27-132 (in Japanese).
20. Pnevmatikos NG, Gantes CJ. Pole selection for structural control using the complex Fourier characteristics of the incoming earthquake. *Structural Control and Health Monitoring* 2007; 14(3):

428-447

21. Pnevmatikos N. Pole placement algorithm for control of civil structures subjected to earthquake excitation. *Journal of Applied and Computational Mechanics* 2017; 3(1): 25-36.
22. Basu B, Nielsen SRK. A multi-modal control using a hybrid pole-placement–integral resonant controller (PPIR) with experimental investigations. *Structural Control and Health Monitoring* 2011; 18(2): 191-206.
23. Ahmadizadeh M, Zare AR. Optimal design of passive control systems using stiffness modification and pole assignment algorithm. *Proceedings of the 15th world conference on Earthquake Engineering* 2012, International Association for Earthquake Engineering; Lisbon, Portugal; 30: 24065-24074.
24. Zare, AR, Ahmadizadeh M. Design of viscous fluid passive structural control systems using pole assignment algorithm, *Structural Control and Health Monitoring* 2014; 21(7): 1084-1099.
25. Wonham WM. *Linear Multivariable Control -A Geometric Approach*. Springer-Verlag, New York; 1979.
26. Hikita H, Koyama S, Miura R. The redundancy of feedback gain matrix and the derivation of low feedback gain matrix in pole assignment. Transactions of the Society of Instrument and Control Engineers 1975; 11(5): 56-60 (in Japanese).

Captions for Tables

TABLE 1 Storey stiffness values for case presented in Figure 7 (Each weight: 1,000 tf, 1st natural frequency: 1.0 Hz)

TABLE 1 Storey stiffness values for case presented in Figure 7
(Each weight: 1,000 tf, 1st natural frequency: 1.0 Hz)

Storey	Solution set 1	Solution set 2
Upper (3rd)	148,310	113,730
Inter (2nd)	196,630	137,710
Lower (1st)	216,940	403,940

(Unit: kN/m)

Captions for Figures

FIGURE 1 3-DOF model for pole allocation

FIGURE 2 Region of solution existence

FIGURE 3 Non-dimensional natural frequencies (b = 2.40)

FIGURE 4 Non-dimensional natural frequencies (b = 2.60)

FIGURE 5 Non-dimensional natural frequencies (c = 3.90)

FIGURE 6 Non-dimensional natural frequencies (c = 4.95)

FIGURE 7 Modal shapes (μ_U = 1, μ_D = 2, b = 2.60, c = 3.90)

FIGURE 8 Useful and practical combinations of target damping ratios (b =2.60, c =3.90)

FIGURE 9 Damping ratios for each storey (b = 2.60, c = 3.90, h_1 = 0.05, h_2 = 0.06-0.10)

FIGURE 10 Damping ratios for each storey (b = 2.60, c = 3.90, h_1 = 0.05, h_2 = 0.11-0.20)

FIGURE 11 Damping ratios for each storey (b = 2.60, c = 3.90, h_1 = 0.10, h_2 = 0.17-0.20)

FIGURE 12 Damping ratio plane

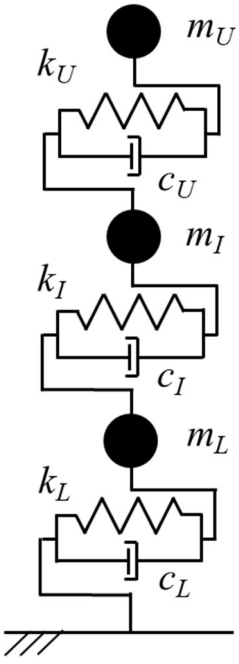

FIGURE 1 3-DOF model for pole allocation

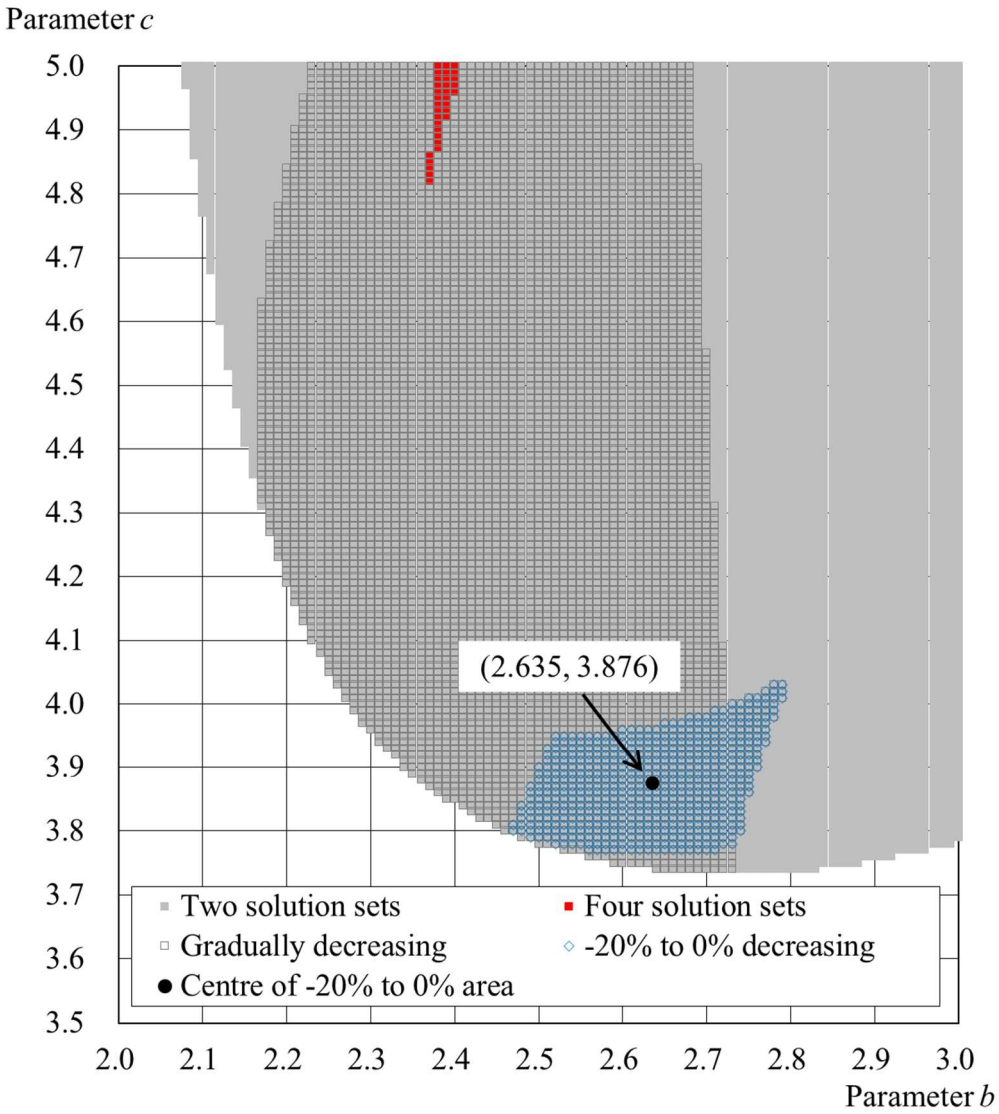

FIGURE 2 Region of solution existence

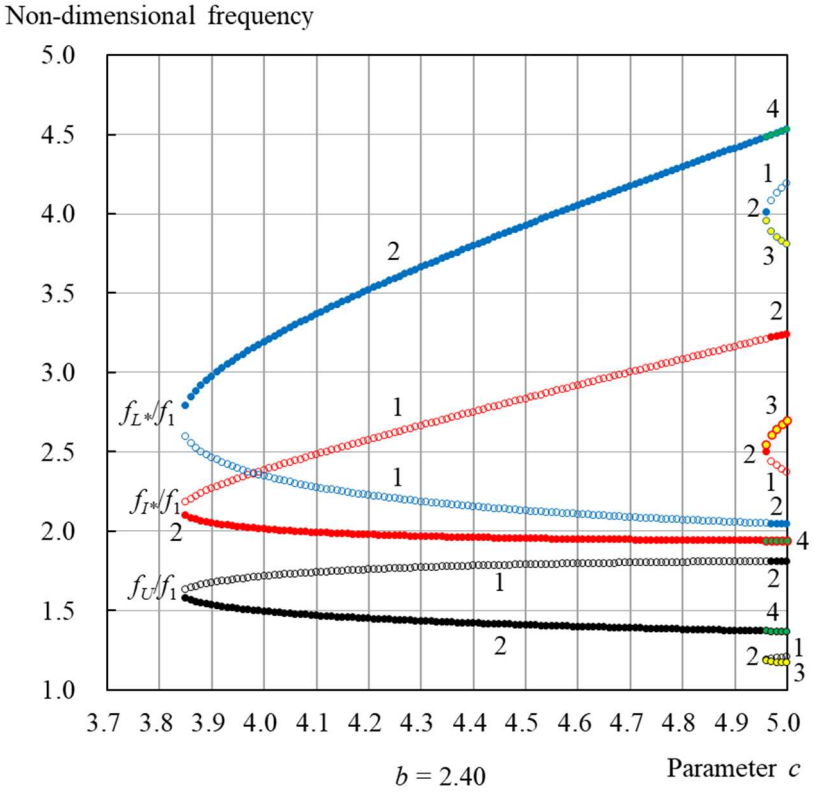

FIGURE 3 Non-dimensional natural frequencies (b = 2.40)

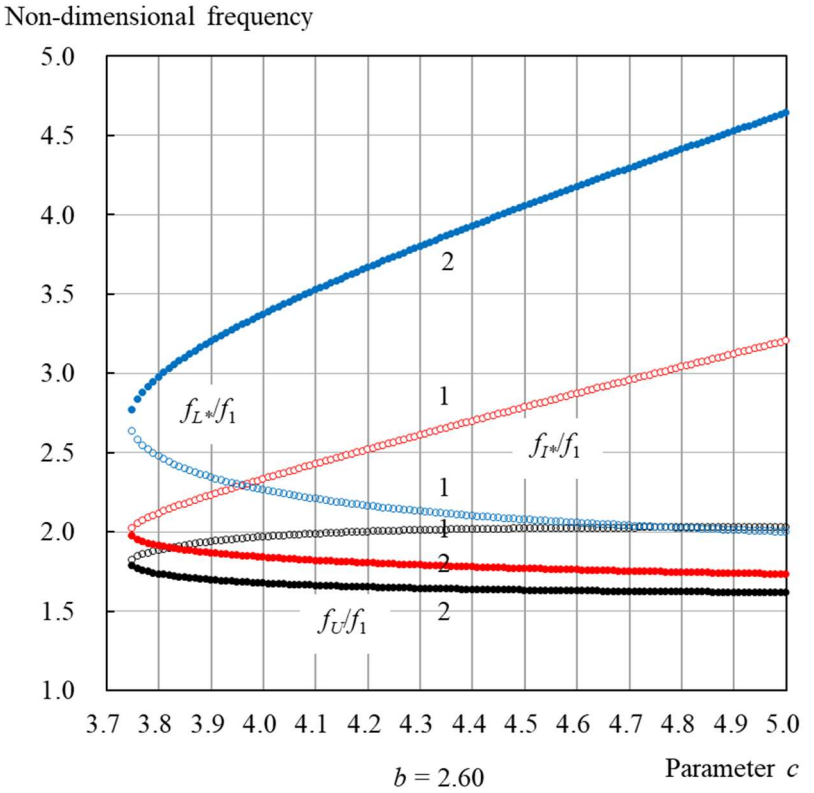

FIGURE 4 Non-dimensional natural frequencies (b = 2.60)

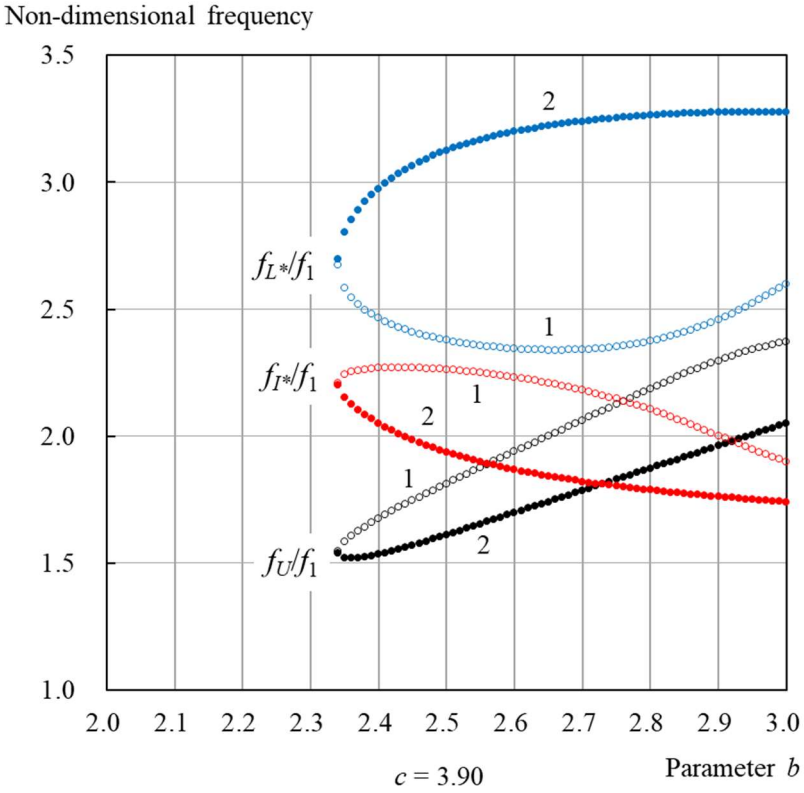

FIGURE 5 Non-dimensional natural frequencies ($c = 3.90$)

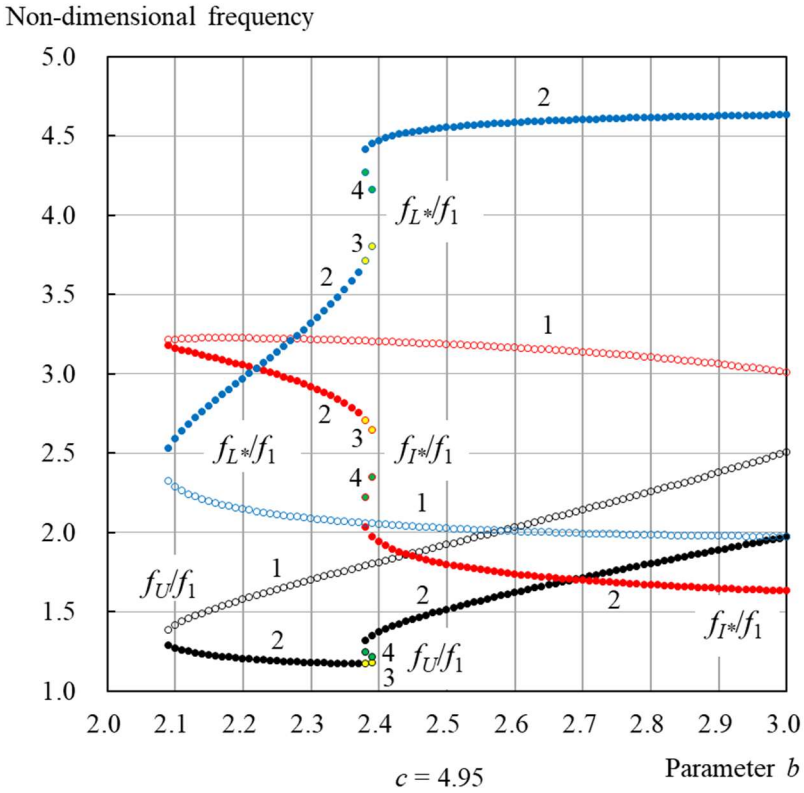

FIGURE 6 Non-dimensional natural frequencies ($c = 4.95$)

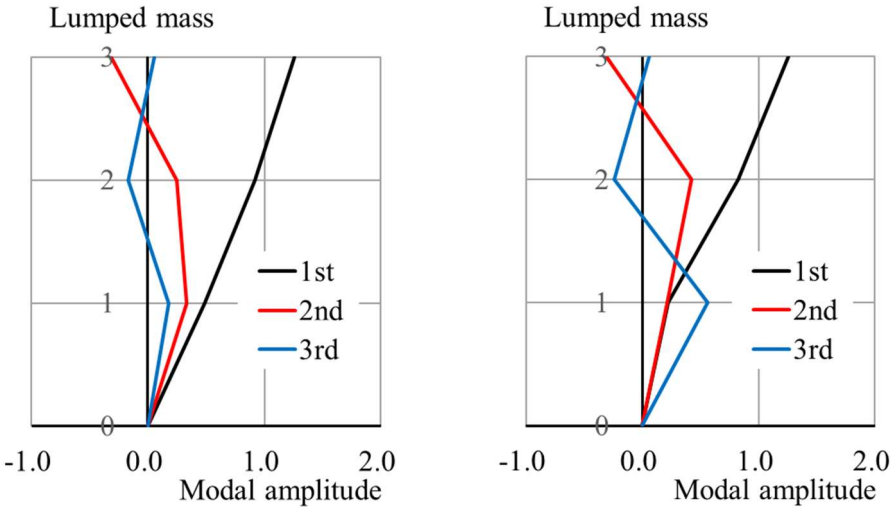

(a) Solution set 1 (b) Solution set 2

FIGURE 7 Modal shapes ($\mu_U = 1$, $\mu_L = 2$, $b = 2.60$, $c = 3.90$)

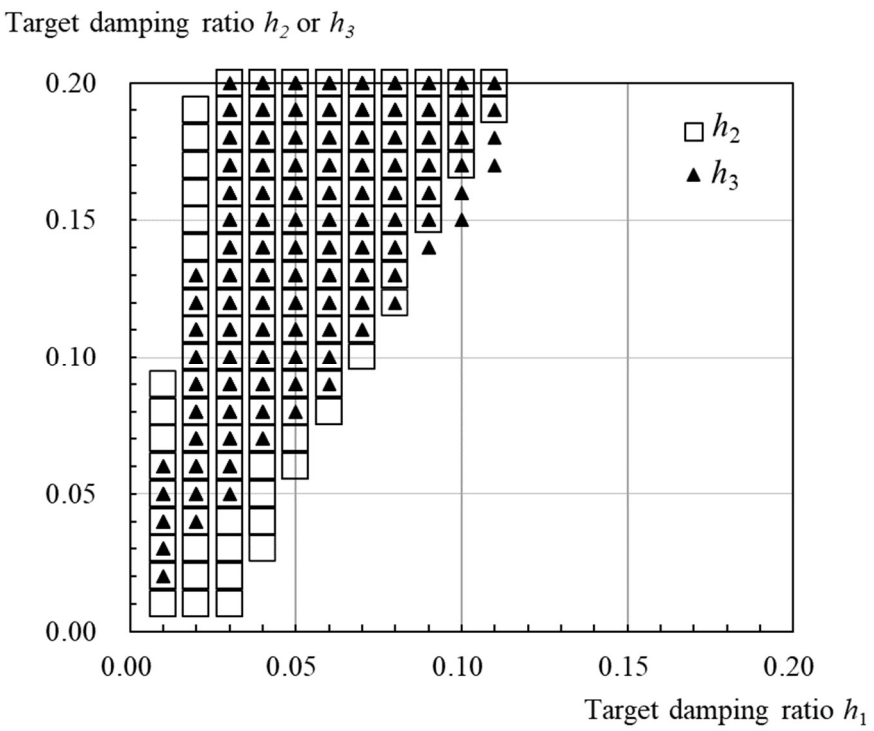

FIGURE 8 Useful and practical combinations of target damping ratios (b =2.60, c =3.90)

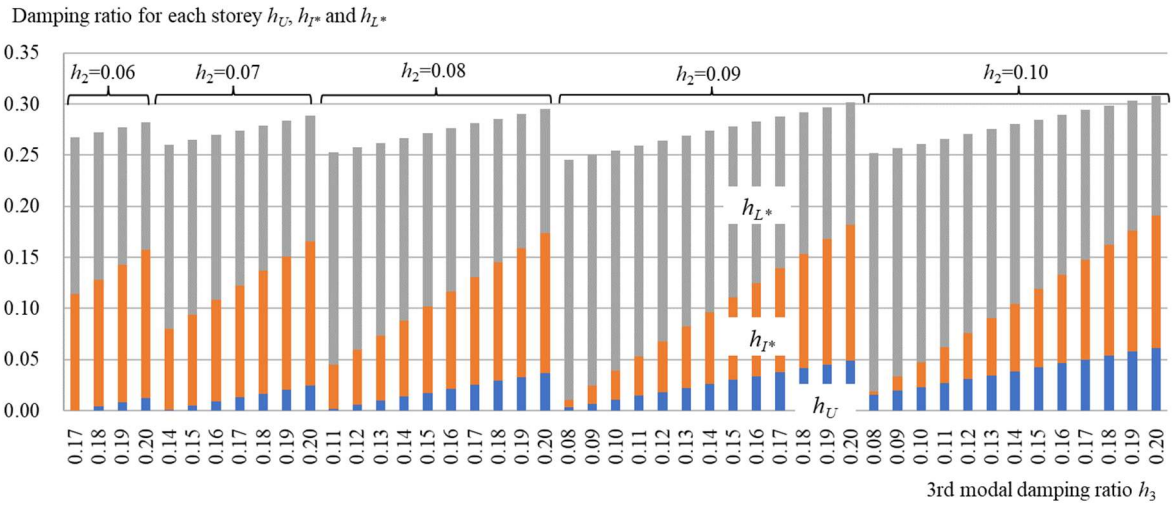

FIGURE 9 Damping ratios for each storey (b = 2.60, c = 3.90, h_1 = 0.05, h_2 = 0.06-0.10)

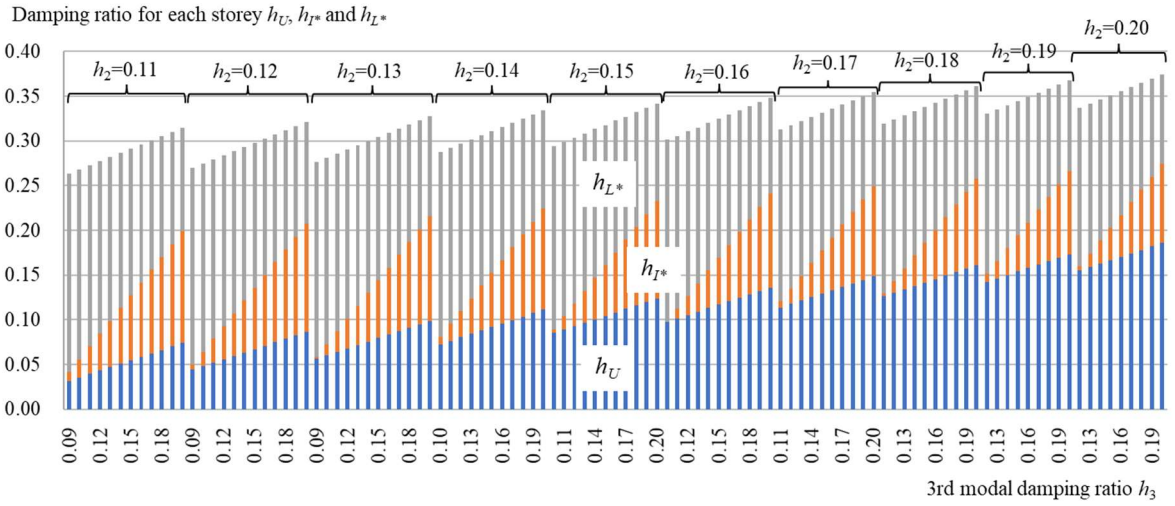

FIGURE 10 Damping ratios for each storey (b = 2.60, c = 3.90, h_1 = 0.05, h_2 = 0.11-0.20)

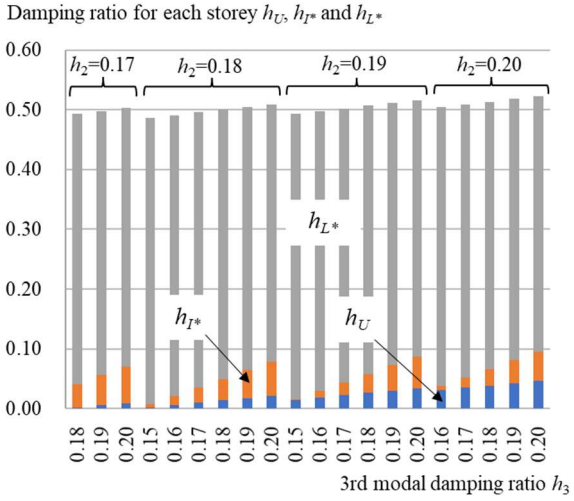

FIGURE 11 Damping ratios for each storey (b = 2.60, c = 3.90, h_1 = 0.10, h_2 = 0.17-0.20)

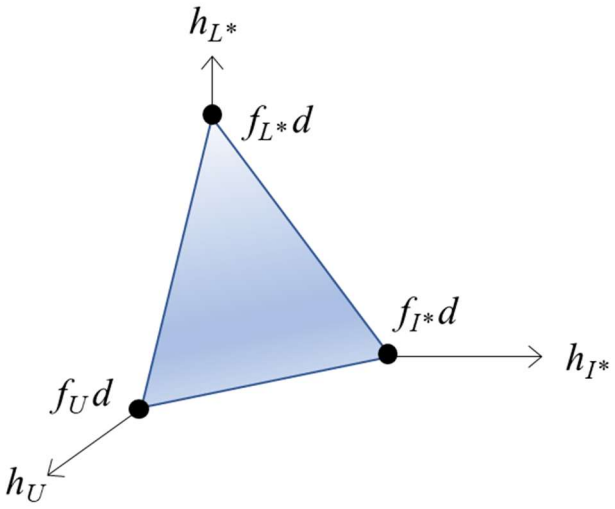

FIGURE 12 Damping ratio plane